

Displacement damage in Hydrogenated Amorphous Silicon p-i-n diodes and charge selective contacts detectors.

M. Menichelli¹, M. Bizzarri^{1,2}, M. Boscardin^{3,4}, L. Calcagnile⁵, M. Caprai¹, A.P. Caricato⁵, G.A.P. Cirrone⁶, M. Crivellari⁴, I. Cupparo⁷, G. Cuttone⁶, S. Dunand⁸, L. Fanò^{1,2}, B. Gianfelici^{1,2}, O. Hammad⁴, M. Ionica¹, K. Kanxheri¹, M. Large¹⁰, G. Maruccio⁵, A.G. Monteduro⁵, F. Moscatelli^{1,9}, A. Morozzi¹, A. Papi¹, D. Passeri^{1,11} *Senior Member IEEE*, M. Pedio^{1,9}, M. Petasecca¹⁰ *Member, IEEE*, G. Petringa⁶, F. Peverini^{1,2}, G. Quarta⁵, S. Rizzato⁵, A. Rossi^{1,2}, G. Rossi¹, A. Scorzoni^{1,11}, L. Servoli¹, C. Talamonti⁷, G. Verzellesi^{3,12}, N. Wyrsh⁸.

Abstract— Hydrogenated amorphous silicon is a well known detector material for its radiation resistance. This study concerns 10 μm thickness, p-i-n and charge selective contacts planar diode detectors which were irradiated with neutrons at two fluence values: 10^{16} $n_{\text{eq}}/\text{cm}^2$ and 5×10^{16} $n_{\text{eq}}/\text{cm}^2$. In order to evaluate their radiation resistance, detector leakage current and response to X-ray photons have been measured. The effect of annealing for performance recovery at 100°C for 12 and 24 hours has also been studied. The results for the 10^{16} $n_{\text{eq}}/\text{cm}^2$ irradiation show a factor 2 increase in leakage current that is completely recovered after annealing for p-i-n devices while charge selective contacts devices show an overall decrease of the leakage current at the end of the annealing process compared to the measurement before the irradiation. X-ray dosimetric sensitivity degrades, for this fluence, at the end of irradiation but partially recovers for charge selective contacts devices and increases for p-i-n devices at the end of the annealing process. Concerning the 5×10^{16} $n_{\text{eq}}/\text{cm}^2$ irradiation test (for p-i-n structures only), due to the activation occurred during the irradiation phase, the results were taken after 146 days of storage around 0°C when a self-annealing effect may have occurred. Nevertheless the results show a degradation in leakage current and x-ray sensitivity which changes very little after annealing.

I. INTRODUCTION

RADIATION damage effects in Hydrogenated Amorphous Silicon (a-Si:H) have been extensively studied in the field of solar panels for space applications like, for example, in the references [1],[2] and [3]. Concerning the radiation resistance for the usage of this material in high energy physics particle detectors, a fundamental reference paper is ref. [4], where a 32 μm thick n-i-p diode has been used for a proton beam monitoring experiment at high fluencies (up to about 10^{16} p/cm^2). The resulting increment in the leakage current of the diode after 7×10^{15} p/cm^2 was measured to be only a factor 2 (crystalline silicon detectors, after more than 20 years of technological R & D, have an increment of leakage current by a factor 50-100 for similar fluencies) and this degradation was completely reversed after 24 hours of annealing at 100 °C. Recovery was also obtained for charge collection efficiency after irradiation and subsequent annealing.

Although a-Si:H has such as remarkable radiation resistance, planar detector fabricated using this material possesses a primary limitation in a poor signal-to-noise ratio for the detection of MIP (Minimum Ionizing Particle) that has yet to exceed the value of 5. The reason for this is the very high voltage needed to deplete a detector (in the order of 10 V/ μm) that generates a very high leakage current that can reach the order of 1 $\mu\text{A}/\text{cm}^2$; additionally the charge collection efficiency is below 50% for a 30 μm thick diode.

A possible solution for these problems is a 3D detector geometry that allows to keep a relatively small inter-electrode distance (in the order of 25-30 μm) with detector thickness around 100 μm in order to increase the total charge generated in the detector by a MIP. The reduction of the distance between the electrodes is a crucial factor for keeping the leakage current low reducing the noise [5,6,7].

One of the main technological challenges in the fabrication of these devices is the doping on the finger type (or trench type) electrodes of the device. The doping techniques to be used in order to solve this problem, should provide a quite uniform coating of the surfaces of the etched cylindrical holes (or trenches). We have found two possible techniques that can fulfill these goals: a) atomic layer deposition of charge selective oxides: MoO_x for hole selective contacts and TiO_2 or

This work was partially supported by the “Fondazione Cassa di Risparmio di Perugia” RISAI project n. 2019.0245.

¹ INFN, Sez. di Perugia, via Pascoli s.n.c. 06123 Perugia (ITALY)

² Dip. di Fisica e Geologia dell’Università degli Studi di Perugia, via Pascoli s.n.c. 06123 Perugia (ITALY)

³ INFN, TIPFA Via Sommarive 14, 38123 Povo (TN) (ITALY)

⁴ Fondazione Bruno Kessler, Via Sommarive 18, 38123 Povo (TN) (ITALY)

⁵ INFN and Dipartimento di Matematica e Fisica “Ennio de Giorgi”

dell’Università di Lecce, Via per Arnesano, 73100 Lecce (ITALY)

⁶ INFN Laboratori Nazionali del Sud, Via S. Sofia 62, 95123 Catania (ITALY)

⁷ INFN INFN and Dipartimento di Fisica Scienze Biomediche sperimentali e Cliniche “Mario Serio”, Viale Morgagni 50, 50135 Firenze (FI) (ITALY)

Aluminum doped ZnO (AZO) for electron selective contacts and b) Ion implantation of Phosphorous (n-type) or Boron (p-type).

In this paper displacement damage radiation testing data using neutrons will be shown. These data were collected during a radiation test performed in the framework of the 3D-SiAm project which has the goal to fabricate and test a-Si:H 3D detectors. The tests here described have been performed using some planar prototype p-i-n and charge selective contacts detectors developed for this experiment.

II. THE TESTED DEVICES AND THE TEST PROCEDURE

Three different device types have been irradiated during this irradiation session: a) Vertical p-i-n diode devices in square pads. b) Vertical p-i-n diode devices in strips c) Vertical charge selective contacts diodes in square pads. Configuration (a) is shown in Fig. 1a, it is a 3×2 diode array of p-i-n vertical diodes where a $10 \mu\text{m}$ layer of a-Si:H is deposited on a p-type crystalline Silicon low resistivity substrate (thickness $300 \mu\text{m}$); on the top of this layer the 6 n-i junctions having $0.5 \times 0.5 \text{ mm}^2$ dimensions are deposited via ion implantation of phosphorous. Passivation with Si_3N_4 and diode metallization with chromium + aluminum is added on the top of the device. The device is then packaged in a ceramic DIL Package (P/N: CSB02219). Configuration (b) (shown in Fig.1b) is an 8-strip device fabricated using the same process described for configuration (a), where the strips have dimensions $5 \times 0.2 \text{ mm}^2$. Configuration (c) (Fig. 1c) has 4 planar charge selective devices each having $4 \times 4 \text{ mm}^2$ surface on a $8.2 \mu\text{m}$ thick a-Si:H substrate; hole selective contact is on top and is molybdenum oxide, the bottom electron selective contact is aluminum-zinc doped oxide (AZO). These detectors have been described in Ref. [8] .

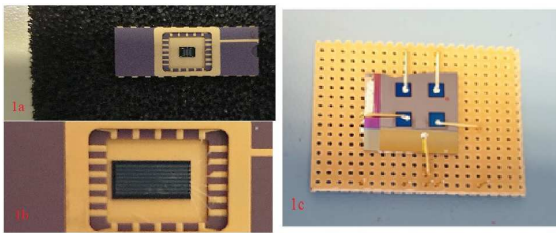


Fig. 1. Detector configurations tested for displacement damage a) Configuration (a) 2×3 pad detector array with n junction implanted and is packaged on a ceramic package b) configuration (b) 8 strip detector with n junction implanted. c) Configuration (c) has 4 charge selective contact devices having $4 \times 4 \text{ mm}^2$ surface and $8.2 \mu\text{m}$ a-Si:H thickness.

The detectors have been irradiated with neutron at the Jozef Stefan Institute in Ljubljana (Slovenia) with two different fluencies of $1 \times 10^{16} \text{ n}_{\text{eq}(1\text{MeV})}/\text{cm}^2$ and $5 \times 10^{16} \text{ n}_{\text{eq}(1\text{MeV})}/\text{cm}^2$, in two different batches.

During the tests, we measured the leakage current at various bias voltages and the detector current under x-ray irradiation at different dose rates. From the linear fit of these data we extracted the dosimetric sensitivity. These measurements were performed for each device: before irradiation, after irradiation and after 12 and 24 hours of annealing. The detectors were biased using a Keithley 2410-C and a Keithley 2400 SMU that measure currents with a 10 pA resolution. X-rays were generated by a tube from Newton Scientific having 50 kV maximum voltage and $200 \mu\text{A}$ maximum current [9], the doses were measured using a Cobia Flex dosimeter equipped with a RTI T20 dose probe [10].

The x-ray test setup is shown in Fig.2 and a typical calibration curve is shown in Fig. 3.

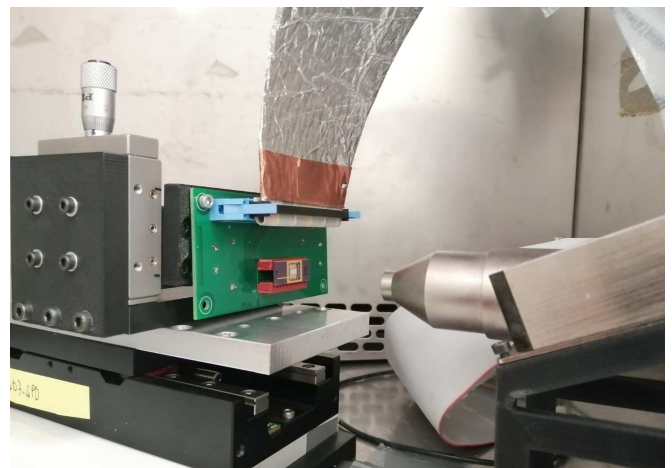


Fig. 2. Test setup for x-ray response measurement.

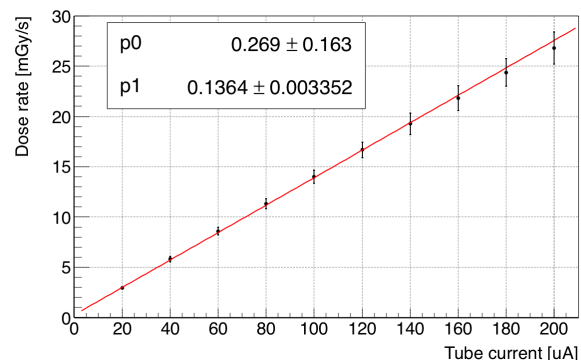


Fig.3 Typical calibration curve between dose and tube current at 30 kV tube voltage. The dose rate was measured by a Cobia Flex dosimeter with the probe placed in the same position of the DUT.

III. RESULTS AFTER $10^{16} \text{ NEQ}/\text{CM}^2$ IRRADIATION

We have tested one configuration (b) and one configuration (c) device after $10^{16} \text{ n}_{\text{eq}}/\text{cm}^2$ neutron irradiation. The neutron spectrum used in this irradiation test is reported in Fig.4.

⁸ Ecole Polytechnique Fédérale de Lausanne (EPFL), Institute of Electrical and Microengineering (IME), Rue de la Maladière 71b, 2000 Neuchâtel, (SWITZERLAND).

⁹ CNR-IOM, via Pascoli s.n.c. 06123 Perugia (ITALY)

¹⁰ Centre for Medical Radiation Physics, University of Wollongong, Northfields Ave Wollongong NSW 2522, (AUSTRALIA).

¹¹ Dip. di Ingegneria dell'Università degli studi di Perugia, via G.Duranti 06125 Perugia (ITALY)

¹² Dip. di Scienze e Metodi dell'Ingegneria, Università di Modena e Reggio Emilia, Via Amendola 2, 42122 Reggio Emilia (ITALY)

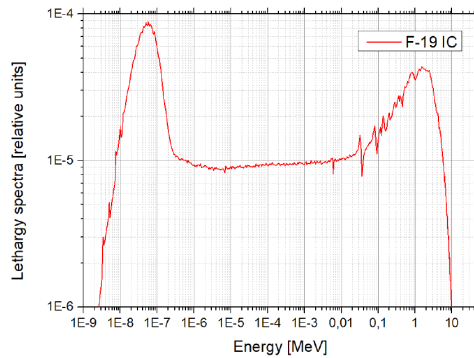


Fig.4 Spectrum of neutron used in this irradiation test [11].

The leakage current was measured for one p-i-n strip diode device and for one charge selective contact device. In Fig.5 the leakage current on p-i-n is shown before and after irradiation and after 12 hours annealing at 100°C as described in the previous chapter. Measurements were performed after 30 minutes of bias at maximum voltage for device current stabilization.

Compared to pre-bias values an increment of leakage current can be observed after irradiation, especially at bias voltages below 70V. After 12 hours of annealing a new measurement was performed and leakage current returned to pre-irradiation values at low bias voltage, becoming even lower at bias voltages higher than 50 V. This is in accordance with what was observed for protons in ref. [4].

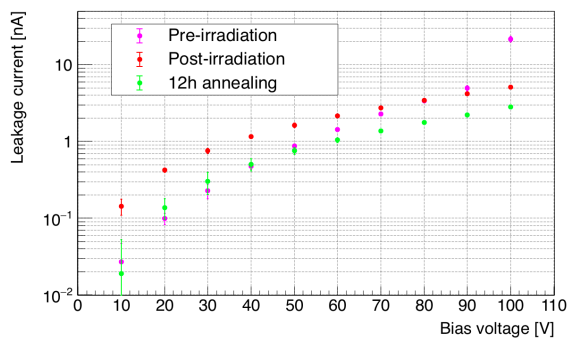


Fig.5 Leakage current versus bias voltage for p-i-n device. The measurement were taken before and after neutron irradiation and after 12 hours of annealing.

The leakage current of charge selective devices was also measured and it is shown in Fig.6. Also in this case we observe an increment of leakage current after the irradiation. The increment was higher at high values of the bias voltage and lower at low bias voltages. In this case two annealing sessions were performed lasting 12 hours each at 100 °C. After the first 12 hours of annealing the values of the leakage current at various voltages were even lower than the pre-irradiation values. The additional 12 hours annealing session basically did not result in any further decrease in leakage current.

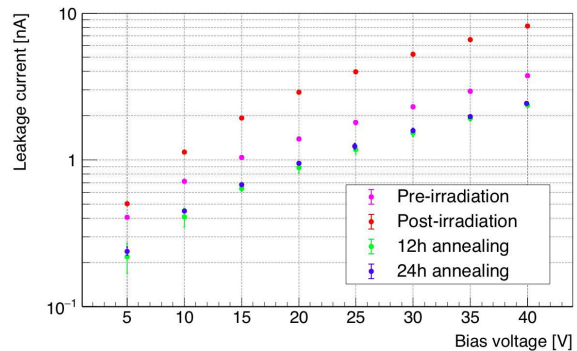


Fig.6 Leakage current versus bias voltage for charge selective contacts device. The measurement were taken before and after neutron irradiation and after 12 and 24 hours of annealing.

Radiation sensitivity and flux response to x-ray irradiation have been measured for these detectors in order to study the response to x-rays and to demonstrate their capability to measure radiation fluxes under severe radiation environments. For this purpose we used the setup shown in fig.2 with the tube biased at 30 kV and dose rates from 0 to 24 mGy/s.

P-i-n diode device biased at 60 V gave the response shown in fig.7. The linearity was very good under all conditions and the sensitivity changed from 2.39 nC/cGy for the non-irradiated component to 1.13 nC/cGy after irradiation; after the 12 hours annealing the sensitivity increased up to 3.0 nC/cGy. This increment is somehow comparable with the leakage current behavior where the leakage current increases after irradiation and decreases below the pre-irradiation value after annealing. It is important to mention that the points of the graph in fig. 7 are obtained measuring the current under x-ray irradiation after subtracting the values of the leakage current. Errors in dose rate are evaluated from the uncertainty of the exact distance between the tube and the detector and for the current we took the standard deviation of measured values.

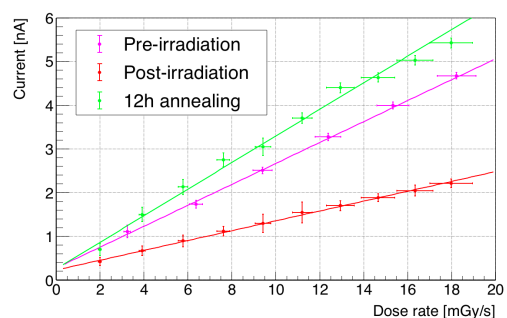


Fig. 7 P-i-n diode device response to x-ray irradiation versus dose rate. The measurement were taken before and after neutron irradiation and after 12 hours of annealing at 100°C.

Charge selective response to x-ray irradiation at various rates has been measured both at 0 V (photovoltaic mode typical of medical dosimetry) bias and at 30 V bias (more suitable for beam dosimetry); the results are shown in Fig. 8 and 9.

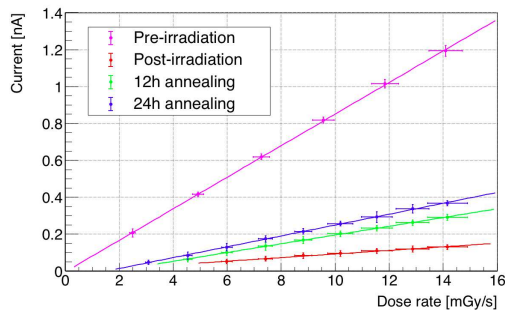


Fig.8 Charge selective contacts device (at 0V bias) response to x-ray irradiation versus dose rate. The measurement were taken before and after neutron irradiation and after 12 and 24 hours of annealing at 100°C

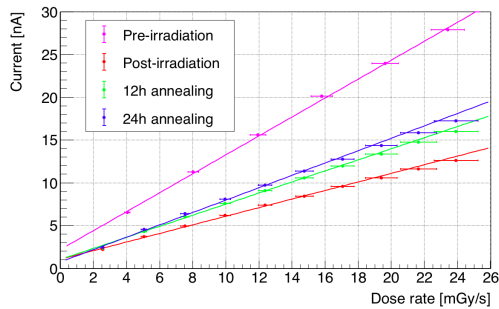


Fig.9 Charge selective contacts device (at 30V bias) response to x-ray irradiation versus dose rate. The measurement were taken before and after neutron irradiation and after 12 and 24 hours of annealing at 100°C.

It should be noted from these data that the recovery after irradiation is less evident than in the p-i-n diode device. Linearity is still quite good especially under bias; however at 0V the charge sensitivity is 0.86 nC/cGy for the non-irradiated component while after irradiation decreases by a factor of 8.6 (0.10 nC/cGy). The device partially recovers after 12 hours annealing up to 0.24 nC/cGy and to 0.30 after 24 hours of annealing. The results obtained with a 30 V bias confirm this trend: the sensitivity before irradiation was 11.1 nC/cGy reducing by more than a factor 2 after neutron irradiation down to 5.0 nC/cGy, it partially recovers after 12 h annealing up to 6.5 nC/cGy and after 24h up to 7.2 nC/cGy. A summary table of these results is shown in Table I.

TABLE I
SENSITIVITY UNDER VARIOUS CONDITIONS FOR P-I-N DIODE AND CHARGE SELECTIVE CONTACTS DEVICES AFTER 10^{16} N_{EQ}/CM^2 NEUTRON IRRADIATION

Detector type and bias	Pre-rad Sensitivity (nC/cGy)	Sensitivity after irradiation (nC/cGy)	Sensitivity after 12h annealing (nC/cGy)	Sensitivity after 24h annealing (nC/cGy)
CSC at 30V bias	11.1 ± 0.3	5.0 ± 0.1	6.5 ± 0.2	7.2 ± 0.2
CSC at 0V bias	0.86 ± 0.03	0.10 ± 0.02	0.24 ± 0.02	0.30 ± 0.02
P-i-n diode at 60V	2.39 ± 0.09	1.13 ± 0.08	3.0 ± 0.1	-

IV. RESULTS AFTER 5×10^{16} N_{EQ}/CM^2 IRRADIATION

One configuration (a) and one configuration (b) p-i-n diode devices were irradiated with 5×10^{16} n_{eq}/cm^2 neutron fluence.

After the irradiation the components were heavily activated and measurements could not take place until after 146 days from the irradiation. Although during this time the components were kept around 0°C some self-annealing has to be considered. This effect can explain why for this measurement the actual annealing at the 100 °C temperature had a reduced effect compared with the measurements described in the previous section. Due to residual activity the components could not be shipped, hence the x-ray response was measured after irradiation and annealing at the JSI laboratory with a different setup. The x-ray tube that was used in Lubljana had a tungsten cathode, voltage in the 5-160 kV range with current in the range 0.5-50 mA and maximum power of 3 kW. Preliminary dosimetric measurements on the JSI setup were performed with the same instrument we used for the measurement described in the previous section for dose rate consistency of the two setups. A picture of the JSI x-ray setup is shown in Fig.10.

The leakage current for one of the configuration (a) devices is shown in Fig. 11. There is a relevant increase (by a factor of 2.5 at 100 V) in leakage current after irradiation that does not change after annealing probably due to self-annealing under storage as already mentioned at the beginning of this section. The larger error bars on the pre-irradiation curve are due to the different (and more noisy) setup used.

Concerning configuration (b) device (Fig.12) we notice a decrease in leakage current after irradiation (and self-annealing). After the 12 hours annealing at 100°C the leakage current increased above the non-irradiated values and did not change significantly after 24 hours of annealing.

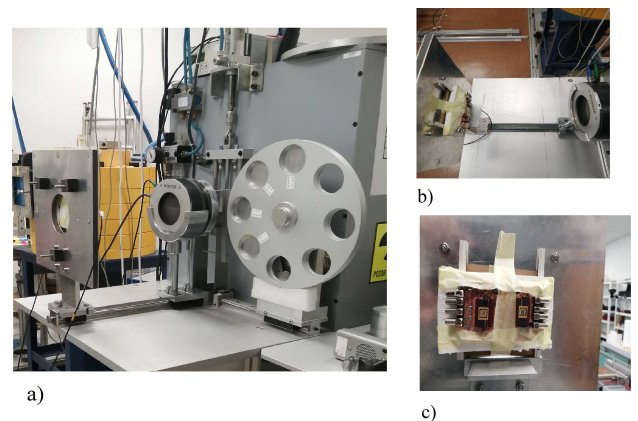


Fig.10 a) X-ray tube at JSI with monitoring ionization chamber and sample holder b) Top view of ionization chamber and sample holder c) samples on the holder irradiated simultaneously.

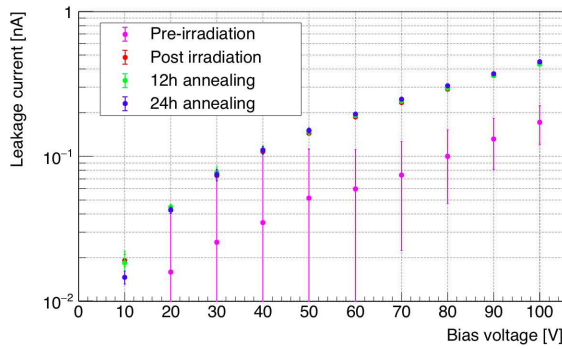


Fig. 11 Leakage current versus bias voltage for configuration (a) device. The measurements were taken before and after neutron irradiation and after 12 and 24 hours of annealing.

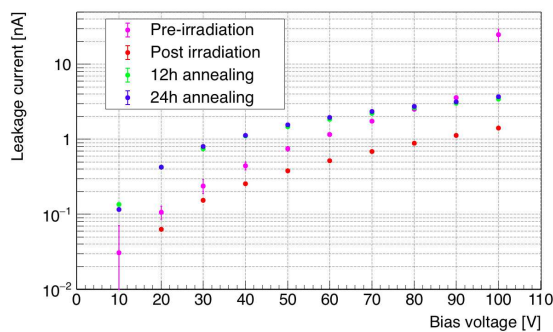


Fig. 12 Leakage current versus bias voltage for configuration (b) device. The measurements were taken before and after neutron irradiation and after 12 and 24 hours of annealing.

X-ray response was measured for both devices. Configuration (a) device (Fig.13) shows good linearity and a reduction of sensitivity from 1.94 to 0.57 nC/cGy after irradiation and auto-annealing. After 12 hours of annealing the sensitivity increased to 0.77 nC/cGy and after 24 hours of annealing increased additionally up to 0.84 nC/cGy.

Also configuration (b) device shows very good linearity (Fig.14). After irradiation and auto-annealing the charge sensitivity was reduced from 2.55 to 0.74 nC/cGy. After 12 hours of annealing the sensitivity increased to 1.07 nC/cGy and after 24 hours of annealing increased additionally up to 1.27 nC/cGy

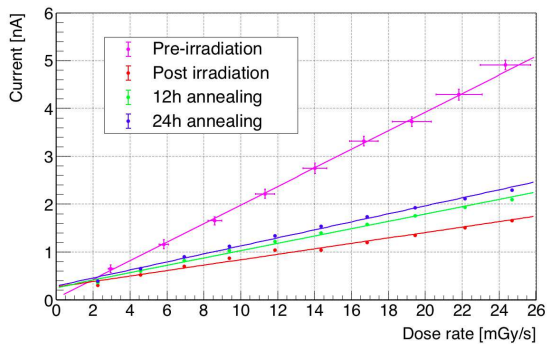


Fig. 13 Configuration (a) device response to x-ray irradiation versus dose rate. The measurement where taken before and after neutron irradiation and after 12 and 24 hours of annealing at 100°C.

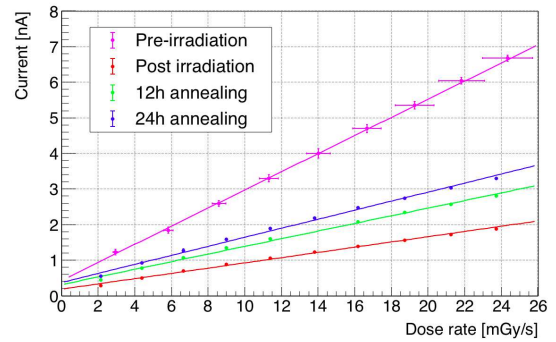


Fig. 14 Configuration (b) device response to x-ray irradiation versus dose rate. The measurement where taken before and after neutron irradiation and after 12 and 24 hours of annealing at 100°C.

A summary table of these measurements is shown in table II.

TABLE II
SENSITIVITY UNDER VARIOUS CONDITIONS FOR CONFIGURATION A AND B DEVICES AFTER 5×10^{16} N_{EQ}/CM^2 NEUTRON IRRADIATION

Detector type and bias	Pre-rad Sensitivity (nC/cGy)	Sensitivity after irradiation (nC/cGy)	Sensitivity after 12h annealing (nC/cGy)	Sensitivity after 24h annealing (nC/cGy)
Configuration a device at 60V bias	1.94 ± 0.07	0.568 ± 0.005	0.769 ± 0.006	0.837 ± 0.006
Configuration b device at 60V bias	2.55 ± 0.08	0.737 ± 0.006	1.07 ± 0.01	1.27 ± 0.01

During sensitivity measurements, we also tested the stabilization of the time response of these devices and we realized that annealing generates a slowdown in detector response. Figure 15 shows detector response with time before/during/after the application of x-ray (24 mGy/s dose rate) irradiation on a configuration (b) device before and after the first 12 hours of annealing. From this figure we can notice that although, after annealing, the pulse amplitude increases in its absolute value, it also shows a slower rise time at turn on (disregarding the spike which is a tube spurious pulse) and a tail after tube turn-off that are not visible on the data taken before annealing.

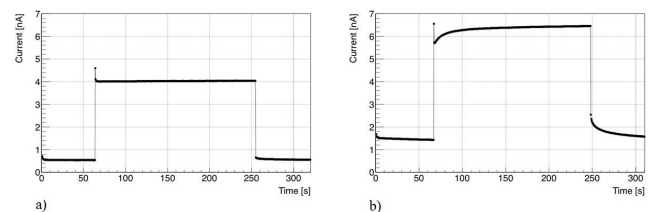


Fig. 15 Time response of the current before/during/after the x-ray irradiation test for a configuration (b) device irradiated with a dose rate of 24 Gy/s a) response of an irradiated and self-annealed device. b) same device after the first 12 hours of annealing.

V. CONCLUSIONS

A total of four a-Si:H detector devices have been irradiated with neutron at the Jozef Stefan Institute reactor facility in Ljubljana (SLO). These detectors were designed in three different configurations:

- **Configuration a** Vertical p-i-n diode devices in square pads ($0.5 \text{ mm} \times 0.5 \text{ mm}$).
- **Configuration b** Vertical p-i-n diode devices in strips ($5 \text{ mm} \times 0.2 \text{ mm}$)
- **Configuration c** Vertical charge selective contacts diodes in square pads ($4 \text{ mm} \times 4 \text{ mm}$)

One configuration (b) and one configuration (c) devices were irradiated up to the total fluence of $1 \times 10^{16} n_{\text{eq}(1\text{MeV})}/\text{cm}^2$ and then annealed for 12 hours (device type (b) and (c)) and 24 hours (device (c) only) at the temperature of $100 \text{ }^\circ\text{C}$. After the irradiation we observe an increment in leakage current more homogeneous at all bias voltages for configuration (c) device and more evident at low bias voltages for configuration (b) device. After 12 hours of annealing the leakage current returned to the original value for the configuration (b) component and was reduced to about 50% for configuration (c) device. The radiation sensitivity under non-zero bias was reduced by more than a factor 2 after irradiation and partially recovered (up to 65%) for the charge selective contact device and had a 25% increment compared to the original value for the configuration (b) device. From these data, we can infer that irradiation generates a visible damage in the two devices, and a partial or total recovery is observed after annealing. Concerning the irradiation of one configuration (a) and one configuration (b) device up to fluencies $5 \times 10^{16} n_{\text{eq}}/\text{cm}^2$ it is important to consider that due to activation the two devices were measured only after 146 days from the end of neutron irradiation and these may have induced some auto-annealing making the successive $100 \text{ }^\circ\text{C}$ annealing less efficient in the recovery of the performances. Nevertheless the two devices, after the 24 hours of annealing, recovered partially their performances. The radiation sensitivity, after the complete annealing process was 43% of the pre-rad value for configuration (a) and 50% for configuration (b). In the near future we plan to repeat the irradiation with protons in the few MeV range, combining the effect of displacement with the effect of total ionizing dose.

ACKNOWLEDGMENT

The authors wish to acknowledge the JSI personnel in particular Dr. Anze Jazbec and Dr. Matjaz Mihelic for their fundamental contribution during activation monitoring and x-ray tests. The p-i-n devices were developed by Fondazione Bruno Kessler (FBK) in the framework of FBK and INFN MiNaTAP agreement on a a-Si:H layer deposited by EPFL. Charge selective contacts devices were fully developed by EPFL.

REFERENCES

- [1] J.R. Srour et al. Damage Mechanism in Radiation-Tolerant Amorphous Silicon Solar Cells. *IEEE Trans. Nucl. Sci.* Vol. 45 pp. 2624–2631 1998
- [2] J. Kuendig et al. Thin film silicon solar cells for space applications: Study of proton irradiation and thermal annealing effects on the characteristics of solar cells and individual layers. *Solar Energy Materials & Solar Cells* Vol. 79 pp. 425–438, 2003.
- [3] H.C. Neitzert et al. Investigation of the damage as induced by 1.7 MeV protons in an amorphous/crystalline silicon heterojunction solar cell. *Solar Energy Materials & Solar Cells* Vol. 83 pp. 435–446 2004.
- [4] N. Wyrsh et al. Radiation hardness of amorphous silicon particle sensors. *J. Non-Cryst. Solids*, Vol. 352, pp. 1797–1800. 2006.
- [5] M.Menichelli et al. Hydrogenated amorphous silicon detectors for particle detection, beam flux monitoring and dosimetry in high-dose radiation environment. *JINST* Vol. 15, N.C04005 2020.
- [6] M.Menichelli et al. 3D Detectors on Hydrogenated Amorphous Silicon for particle tracking in high radiation environment. *J. Phys.: Conf. Ser.* Vol. 1561 N.012016 2020
- [7] M.Menichelli et al. Fabrication of a Hydrogenated Amorphous Silicon Detector in 3-D Geometry and Preliminary Test on Planar Prototypes. *Instruments*, Vol. 5, N. 32. 2021.
- [8] M.Menichelli et al. Testing of planar hydrogenated amorphous silicon sensors with charge selective contacts for the construction of 3D detectors. *JINST* 17 C03033 2022
- [9] Datasheet available at <http://www.newtonscientificinc.com/50kv-10w-monoblock/> Last accessed 3rd Fe. 2022
- [10] Specifications available at <https://rtigroup.com/products/cobia-rti-cobia-flex-r-f/#specification> Last accessed 3rd Feb. 2022
- [11] A. Jazbeck private communication.